Journal of
Materials Chemistry A

Accepted Manuscript

This article can be cited before page numbers have been issued, to do this please use: S. P V, B. N. Nair, A. M. Peer, G. M. Anilkumar, K. G. Warrier, T. Yamaguchi and H. U. N. Saraswathy, *J. Mater. Chem. A*, 2016, DOI: 10.1039/C6TA06133H.

ROYAL SOCIETY OF CHEMISTRY

www.rsc.org/materialsA

View Article Online
DOI: 10.1039/C6TA06133H

Journal Name

ARTICLE

Morphologically and compositionally tuned lithium silicate nanorods as high-performance carbon dioxide sorbents.

Received 00th January 20xx,
Accepted 00th January 20xx

DOI: 10.1039/x0xx00000x

www.rsc.org/

P. V. Subha[a], Balagopal N. Nair[*b,c], A. Peer Mohamed[a], G. M. Anilkumar[b], K. G. K. Warrier[a], T. Yamaguchi[d] and U. S. Hareesh[*a,e]

The effective capturing of carbon dioxide using regenarable high capacity sorbents is a prerequisite for industrial applications aiming CO_2 capture and sequestration. The removal of CO_2 directly from the chemical reaction environments at high temperature is a less energy intensive method of its separation with the added benefit of improved efficiency in equilibrium limited reactions. However, the separation of CO_2 at the typical reaction temperatures of 573-1073 K is a challenging task, due to the non-availability of absorbents with kinetics comparable to reaction rates. Moreover their poor durability due to sintering and particle growth on prolonged use at the high temperature is also an impediment to practical applications. Herein, we demonstrate the development of an efficient CO_2 absorbent material, made of Li_4SiO_4 nano rods, with ultrafast sorption kinetics as well as remarkable durability. These nano rods enabled easier surface reaction with CO_2 due to shorter diffusion pathway for lithium from the bulk to surface of the rods permitting extremely fast absorption of CO_2. Furthermore, the compositional tuning of the materials helped to realize absorbents with extraordinary CO_2 absorption rates of 0.72 wt % sec^{-1} at 100% CO_2/923K. The exceptional performance of these absorbents at lower temperatures (573-823K) as well as lower CO_2 pressures (0.15 atm) demonstrates their potential in practical CO_2 separation applications.

1. Introduction

Global warming and its effect on climate destabilization have grown into an alarming environmental concern in recent times. The massive consumption of fossil fuels leading to vast greenhouse gas emissions, since the industrial revolution is believed to be the major reason for the current rise in atmospheric temperature. Green technological alternatives based on wind, solar and hydropower plants are therefore favored for minimal carbon footprints in the atmosphere. However, considering the cost and time frame required for the widespread implementation of such renewable energy alternatives, an immediate solution appears remote. To reduce carbon footprints globally, a reduction in CO_2 emission by maintaining a balanced carbon cycle in the atmosphere is imperative. Selective greenhouse gas capture and separation for reuse or sequestration thus emerge as a viable choice to limit its emission to the atmosphere[1]. Among the strategies designed, CO_2 capture using sorbents with appreciable absorption capacity, enhanced kinetics, selectivity, durability and cyclic stability together with minimum energy penalty on the process appears practically viable at least in the short-term[2-6].

Removal of CO_2 at high temperatures is an effective option to reduce its emissions to the atmosphere[7-9]. In several high-temperature chemical and petrochemical processes, CO_2 is a

[a] Materials Science and Technology Division (MSTD), National Institute for Interdisciplinary Science and Technology, Council of Scientific and Industrial Research (CSIR-NIIST), Pappanamcode, Thiruvananthapuram, Kerala 695019, India. *E-mail: hareesh@niist.res.in
[b] R&D Centre, Noritake Company LTD, 300 Higashiyama, Miyoshi, Aichi 470-0293, Japan. * E-mail: bnair@n.noritake.co.jp
[c] Nanochemistry Research Institute, Department of Chemistry, Curtin University, GPO Box U1987, Perth, Western Australia 6845, Australia
[d] Chemical Resources Laboratory, Tokyo Institute of Technology, Nagatsuta 4259, Midori-ku, Yokohama 226-8503, Japan
[e] Academy of Scientific and Innovative Research, Delhi–Mathura Road, New Delhi 110 025, India
† Supplementary Information (ESI) available: [Experimental and supplementary figures and tables included]. See DOI: 10.1039/x0xx00000x

View Article Online
DOI: 10.1039/C6TA06133H

major product and its removal therefore at the temperature and pressure of the reaction offers a less energy intensive method of separation culminating in smaller carbon footprints. In reactions such as methane reforming, the removal of CO_2 from the reaction vessel could also enhance the rate of reaction (Sorption Enhanced Steam Reforming) providing thereby additional benefits of increased productivity[10-11]. However, selective and rate enhanced sorption of CO_2 at elevated temperatures is a challenging task, especially in the temperature range of 573-1073 K where most such reactions occur. Lithium based ceramic absorbents are considered as candidate materials for selective CO_2 removal at high temperature[12-15], although their application is thus far limited by the slow kinetics at the lower temperature range (573-823K) and poor material durability at the higher temperature range (823K-1073K).

Among the lithium ceramics, lithium silicate (Li_4SiO_4) based ceramic oxides are the most efficient CO_2 sorbents by virtue of their high absorption capacity, faster kinetics and reasonable durability[16-19]. The absorption properties of some of the recently published lithium-based ceramic absorbents are shown as Table S1 in section S1 of the Supplementary Information [20-25] for a quick evaluation of the status. We also have reported on the sol-gel based synthesis of Li_4SiO_4 particles (powders termed as sol-gel in this manuscript) with CO_2 absorption performance comparable to such published reports[26]. In the work reported herein, we have adapted a facile microwave assisted sol-gel synthesis route[27,28] to successfully realize Li_4SiO_4 nano-rods with significantly superior CO_2 absorption performance. Detailed synthesis protocol starting from $LiNO_3$ and colloidal silica is described under methods section. The powders thus obtained exhibited excellent CO_2 absorption capacity, cyclic stability and superior absorption/desorption rates (powders termed as microwave sol-gel in this manuscript). We believe that the enhanced kinetics for CO_2 absorption arises from the very small thickness (20 to 30 nm) of rod-shaped Li_4SiO_4 particles. Irrespective of the nano-size, the large aspect ratio of the particles provided them with better stability against aggregation at high working temperatures thereby providing improved durability for a large number of absorption/desorption cycles. Besides this, the compositional control of these morphologically tuned materials helped to realizenovel eutectic compositions containing Na & K as new generation CO_2 absorbents with exceptionally high CO_2 absorption rates even at low and moderate temperatures (< 723 K).

2. Experimental

2.1 Synthesis of Li_4SiO_4 through microwave sol-gel process.

Li_4SiO_4 was synthesised from $LiNO_3$ (Alfa Aesar, UK) and colloidal silica (Aldrich Chemicals, USA) as starting precursors. Initially 2.39 M $LiNO_3$ solution was prepared by dissolving it in distilled water. Hydrolysis was carried out by the addition of NH_4OH to $LiNO_3$ solution while stirring at room temperature. Colloidal silica was added drop wise under stirring for 1 hour to obtain a sol. The precursor sol was subjected to a 700 W microwave radiation at 2.45 GHz for 10 min. A domestic microwave oven (Panasonic-NNGT231M) was used to carry out this experiment. The precursor was then dried at 423K and heated to 1073K at a ramp rate of 1°C/min in air atmosphere. The powder calcined at 1073 K for 3 hours was used for CO_2 absorption studies unless specified otherwise.

2.2 Processing of the mixture of Li_4SiO_4 and alkali carbonates

Na_2CO_3 (99.9%), K_2CO_3 (99.8%) and Li_2CO_3 (98%) all from Merck, India were mixed in the weight ratio of 10:60:30 [eutectic -1], 32:37:31 [eutectic-2] and 24:45:31 [eutectic–3] and then blended with the microwave sol-gel samples in the weight ratio 1:5. The mixtures were then heat treated at 1073 K before the absorption studies at various temperatures.

View Article Online
DOI: 10.1039/C6TA06133H

2.3 Characterization techniques

Phase changes of the powder samples during heat treatment were traced using insitu HT-XRD (Rigaku RINT-TTR III). The morphology and crystallinity of the powders on CO_2 absorption/desorption were further characterised using TEM analysis (HRTEM, FEI Tecnai 30 G2 S-TWIN operated at an accelerating voltage of 300 kV). CO_2 absorption properties were measured using a TGA apparatus (Perkin Elmer STA 6000, Singapore), in the temperature range of 100-750 °C. N_2 adsorption based surface area analysis was performed at 77K using Micromeritics Tristar 111 surface area analyser after degassing the sample at 200 °C for 2 h.

3. Results and discussions

Morphological features of the synthesized particles at 673K, 773K and 1073 K are observed by TEM and are shown in Fig. 1 (a-f). Remarkably, TEM images show that the particles are of nano rod morphology and are entirely different from the powders synthesized by conventional processing techniques[29,30]. The XRD patterns of the microwave sol-gel Li_4SiO_4 samples after heat treatment (calcination) at 673K, 773K and 1073 K are further presented in Fig. 1g. From the XRD results, it is clear that the particles exhibited amorphous nature even after calcination at 673 K. Crystalline phases rich in Li_2SiO_3 phase emerged only on increasing the temperature to 773K. Heat-treatment at 1073 K was essential to realize Li_4SiO_4 phase (JCPDS file no.37- 1472) rich powders. The temperature dependent phase formation of the powders during heat treatment of the synthesized particles has also been traced using in situ HT-XRD analysis and the results are detailed in section S2 of supplementary Information. Results presented in Fig. 1g and further in supplementary section S2 clearly revealed that the formation of Li_4SiO_4 phase is achieved at the expense of Li_2SiO_3 nano fibers that are initially nucleated from the amorphous silica particles coated with the lithium species. From XRD analysis (Section S2, Figure S1 of the supplementary section), it was inferred that microwave treatment has influenced the hydrolysis of $LiNO_3$ to LiOH. We believe the formation of LiOH phase during hydrolysis and further the intermediate formation of Li_2SiO_3 fibers are critical steps in the successful formation of the Li_4SiO_4 nano rods (Please see section S2 of the supplementary information and the figures and video in the section for a detailed explanation of the phase and morphology formation mechanism). Small peaks corresponding to Li_2SiO_3 phase are visible in Fig. 1g as well as Fig. S2 (supporting information). Usually, such presence of the Li_2SiO_3 phase in small quantities is considered to be due to the reaction between Li_4SiO_4 and CO_2 in air[1, 26] while cooling after heat-treatment or handling during XRD measurements. However, the presence of Li_2SiO_3 peaks in Fig. S2 (in situ XRD spectra) indicate the existence of some amount of the lithium metasilicate phase in our samples.

Based on the XRD and TEM results, 1073 K was used as the calcination temperature for obtaining samples with Li_4SiO_4 as the predominant phase in our study. Unless otherwise mentioned samples named as "microwave sol-gel" in this manuscript are calcined at 1073K. The BET surface area analysis indicated a value of 7.3 m^2/g (N_2 adsorption isotherm is shown in section S3 of supplementary) for the particles.

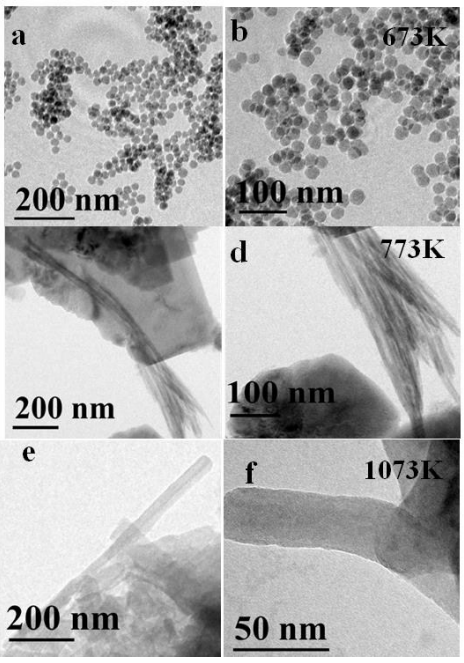

View Article Online
DOI: 10.1039/C6TA06133H

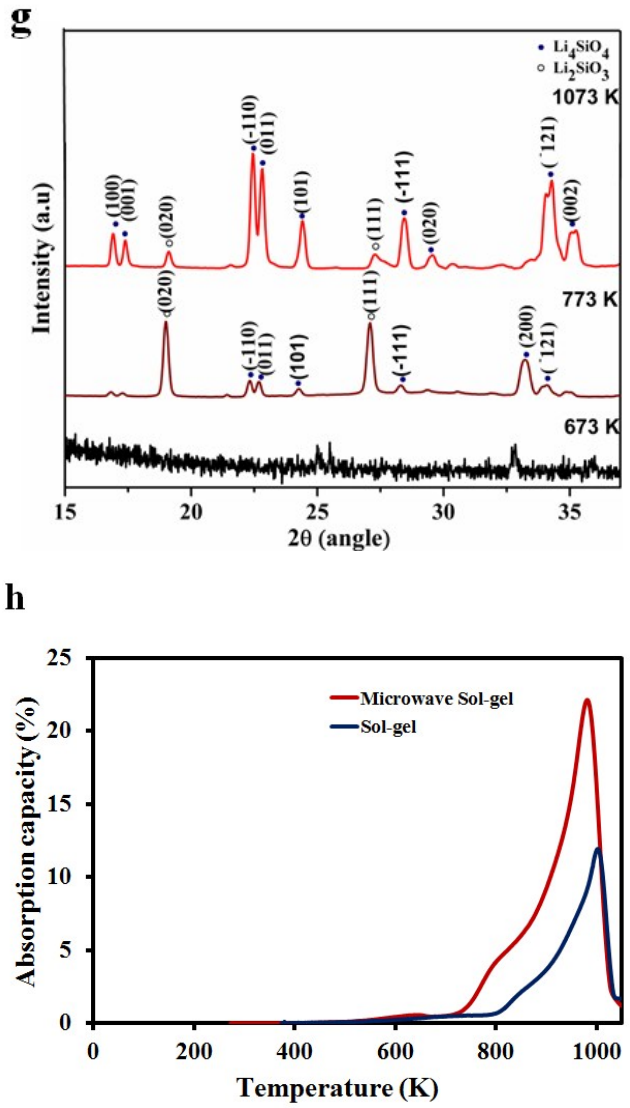

Fig.1 TEM images of particles calcined at 673 K (a & b), 773 K (c & d) and 1073 K (e & f). (g) XRD patterns of Li_4SiO_4 particles synthesized by microwave sol-gel approach after calcination at temperatures of 673K, 773K and 1073K (Li_4SiO_4 * JCPDS 37- 1472), (Li_2SiO_3° JCPDS 29-0828). (h) Dynamic absorption curves of the microwave sol-gel powders in comparison to sol-gel Li_4SO_4 powders, measured at 20 °C/min (100% CO_2)

We have initially performed a dynamic thermogravimetric analysis of microwave sol-gel Li_4SiO_4 particles under 100% CO_2 flow to determine the temperature range of gas absorption (Fig. 1h). For comparison, similar curves of powder samples prepared by the sol-gel method as reported elsewhere[26] is also shown in Fig. 1h. As is clear from the dynamic absorption curves, the microwave sol-gel sample exhibited significant CO_2 absorption capacity in the temperature range of 673-973 K. The absorption is initiated at around 673 K leading possibly to the formation of an external shell of lithium carbonate (Li_2CO_3) on the particle surface. This shell formation remained the main mechanism of absorption up to a temperature of about 823 K. It is also evident from the figure that the rate of absorption increases at around 823 K and remains high till the reversible reaction occurs (~ 993 K). The faster rate of absorption from 823 K is presumed to be due to the softening of the Li_2CO_3 shell, thereby decreasing the kinetic limitations imposed by the solid shell at lower temperatures (*7*). As mentioned, at T>993 K Li_4SiO_4 phase become stable, leading to the complete desorption of CO_2. The absorption studies have thus confirmed that the microwave samples have superior CO_2 absorption performances compared to sol-gel samples in the entire range of temperatures measured.

Morphological features of the microwave sol-gel based particles after CO_2 absorption are shown in Fig 2(a & b). Compared to the original particles that exhibited rods of 20 to 30 nm width [Fig. 1(e & f)], the particles after CO_2 absorption appeared entirely different. As shown in Fig. 2(a & b), the carbonate formation leads to the aggregation of the particles during the absorption stage. It can be inferred that the carbonate-rich particles, easily coalesce together forming a shell around a number of particles in the near vicinity, developing in to an aggregate structure. However, desorption of CO_2 leads to the reversible formation of individual Li_4SiO_4 particles, morphologically similar to the original samples Fig. 2(c &d). The morphological integrity of the particles after CO_2 desorption process clearly evidence the stability of the nano-structures on CO_2 absorption/ desorption cycle. The XRD patterns of the samples before and after CO_2 absorption as well as after desorption are included in section S4 of supplementary for further analysis of the CO_2 absorption/desorption process.

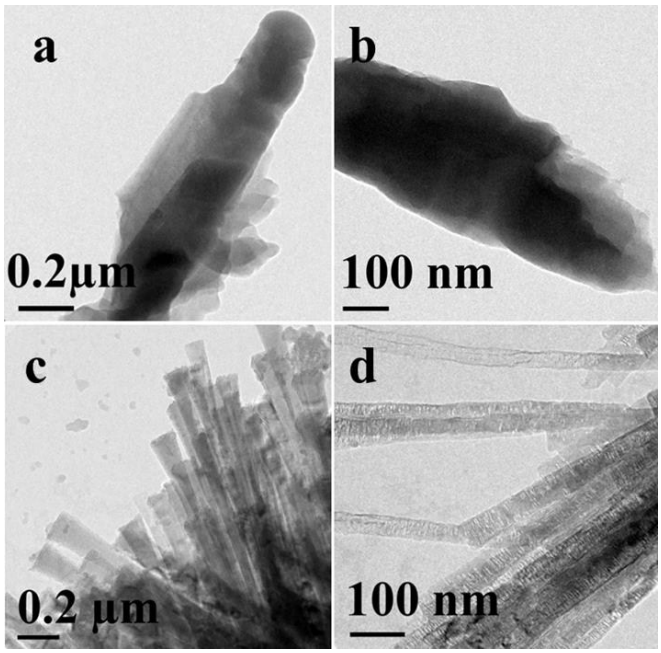

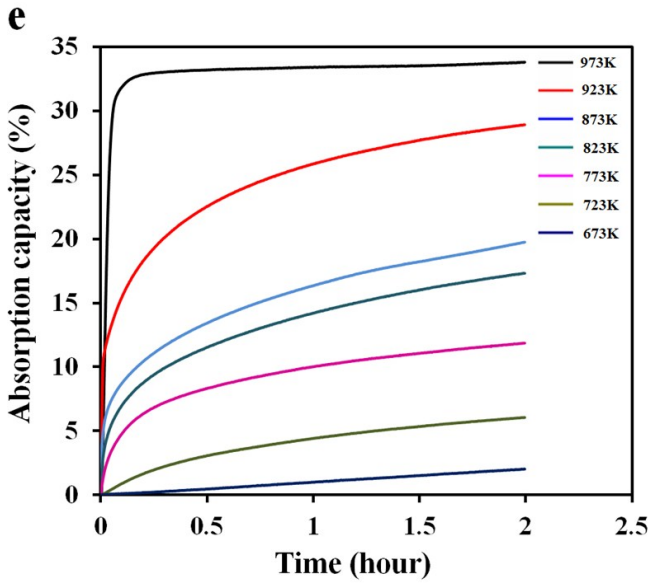

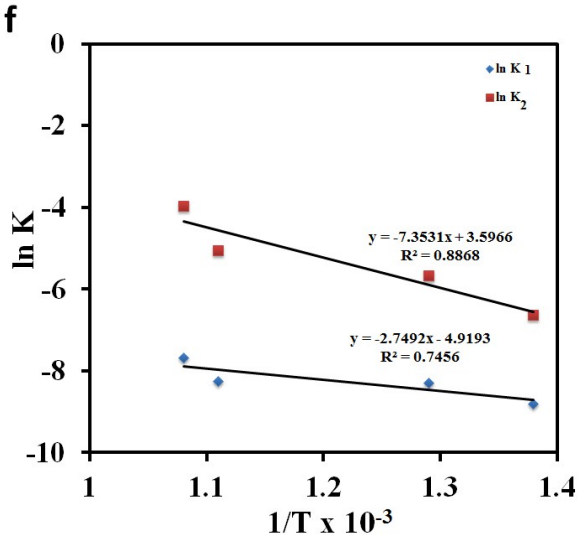

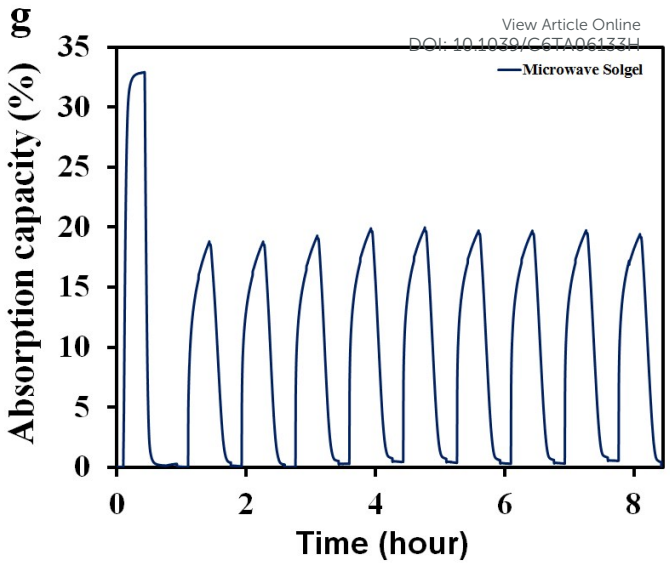

Fig. 2 TEM images (a, b) of microwave sol-gel Li_4SiO_4 particles after CO_2 absorption process (c, d) particles after desorption process. (e) CO_2 absorption curves at various temperatures. (f) Graph of lnK versus 1/T for the two different processes of chemisorption (K_1) and diffusion (K_2) observed in the microwave sol-gel sample (g) Absorption-desorption performance of microwave sol-gel Li_4SiO_4 powders for 10 cycles. The first cycle of the run was done at 973 K and further runs at 873 K. In all cases, desorption was carried out by switching 100% CO_2 gas to 100% N_2 gas.

The CO_2 absorption capacity values of the particles in the temperature range of 673-973 K are compared in Fig. 2e. For collecting the absorption data, the samples were heated to the absorption temperature at 10 ºC min^{-1} in 100% N_2 gas and kept for 2 h under 100% CO_2 gas flow. As expected, the amount of CO_2 absorbed was found increased with increase in absorption temperature. This relation between temperature and absorption capacity as well as the mechanism of absorption are better expressed using kinetic constants and activation energy values calculated from the Arrhenius plots of kinetic constants as in Fig. 2f. Further details on the calculation of kinetic constants are included in section S5 of supplementary. It should be noted that, contrary to the general trend, Fig.2f indicated that the K_2 values are approximately 10 times larger than that of K_1. Larger K_2 values obtained here signifies, faster lithium ion diffusion to the reaction interface compared to the chemisorption reaction[29]. The activation energy values calculated from the plots were 22.70 kJ/mol for the chemisorption

View Article Online
DOI: 10.1039/C6TA06133H

process (corresponding to K_1) and 61.10 kJ/mol for the diffusion process (corresponding to K_2). The higher activation energy value for the diffusion process substantiated the extremely fast diffusion of lithium ions from the core of the material to the reactive interface at absorption temperatures.

Absorption rates were also calculated from the first two minutes of absorption curves at different temperatures. The particles synthesised through microwave sol-gel method displayed enhanced absorption rate of 0.093 wt % sec^{-1} at 973K. This value is much higher than the values reported in the recent literature (See table in supplementary S1 for a comparison of some of the reported values). This enhanced absorption rate should mainly be attributed to the nano-rod morphology characterized by a very small thickness/width of the particle, facilitating a rapid surface carbonate layer formation over the entire length during the first stage of absorption. Moreover, the rod morphology should also have enabled easier surface reaction providing a shorter diffusion pathway for lithium from the bulk to surface of the particle.

Cyclic stability and regenerability of the powder samples were evaluated through cyclic absorption-desorption measurements and results are shown in Fig. 2g [Absorption with 100% CO_2 and desorption with 100% N_2 gases]. The primary aim of this cyclic loading experiment was to examine whether the sintering of the particles or the segregation of carbonate phase due to continuous use of the absorbent at high temperatures induced any decay in absorption performance. Initial absorption run was done at 973 K; thereafter the temperature of absorption was switched to 873 K and cyclic absorption-desorption performance for 9 consecutive cycles was recorded. The initial run at high temperature leading to more or less full conversion of the material to Li_2CO_3 and further to Li_4SiO_4 phase helped to realize higher absorption values at 873K (Fig. 2e and 2g). As shown in Fig. 2g the samples displayed consistent absorption-desorption performance for all the 10 cycles measured indicating high durability and cyclic stability of the materials. Furthermore, it should be noted that desorption rate was better than the absorption rate all through the measurements. The large desorption rate obtained without thermal cycling would allow the application of the materials for CO_2 capture in pressure swing mode. Although, further cyclic studies of thousands of cycles may be necessary before considering the material for real life applications, initial results as reported in Fig. 2g indicated that the microwave sol-gel powders may be considered as promising materials for industrial absorption applications. Schematic illustrations comparing the carbon dioxide sorption and desorption mechanisms of Li_4SiO_4 nanoparticles and the newly developed nano rods, as well the influence of particle morphology on their durability are provided in Fig. 3(a & b). The small thickness of the nanorods enables fast absorption kinetics just as in the case of nanoparticles. The better durability of the nanorod sample is highlighted based on ceramic sintering and particle coalescence mechanisms. It is well known that in liquid phase assisted sintering, the densification is achieved by the rearrangement and shape changes of the particles. Rearrangement is strongly affected by the size and morphology of the particles. Spherical and mono-dispersed particles are advantageous for particle rearrangement and sintering while particles like nano rods having high aspect ratio are difficult to sinter. The Ostwald ripening/particle coalescence process invariably results in a reduction of total surface area of the particles [31,32]. Hence the particle coarsening process as per Fig. 3 b of the schematic always leads to a reduction in absorption kinetics owing to the reduction of absorbent-gas interface available for chemisorption. On the contrary, the use of higher aspect ratio Li_4SiO_4 nano rods impede coalescence and agglomerate formation due to which it is possible to maintain high absorption kinetics even after several absorption/desorption cycles. These effects of morphological tuning on the kinetics of carbon dioxide absorption process as well as durability of the resulting particles are depicted in the illustration shown

View Article Online
DOI: 10.1039/C6TA06133H

in Fig 3. The effects of morphological tuning on the kinetics of carbon dioxide absorption process as well as durability of the resulting particles are clearly depicted in the illustration.

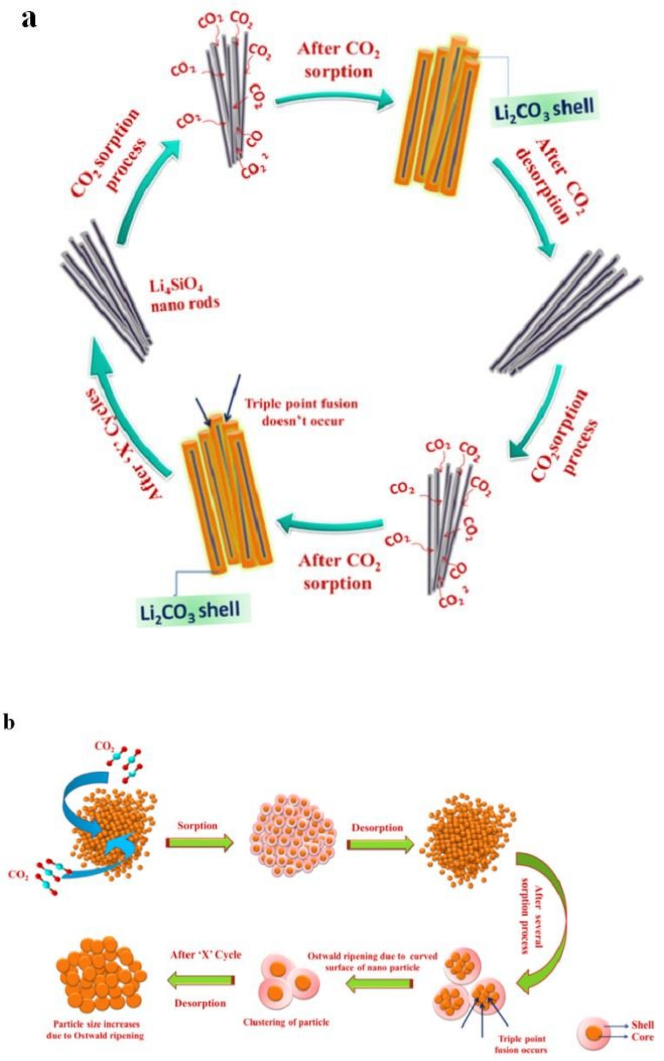

Fig. 3 Schematic illustrations comparing the carbon dioxide absorption and desorption mechanism and durability of (a) the newly developed Li_4SiO_4 nano rods and (b) commonly found Li_4SiO_4 nanoparticles

Further, we tried to enhance the rate of absorption as well as absorption capacity of the materials in the low-temperature range by modifying the materials with a eutectic composition of mixed alkali carbonates. Carbonates of sodium, potassium and lithium were mixed in the weight ratio of 10:60:30 [Eutectic-1], 32:37:31 [Eutectic-2] and 24:45:31 [Eutectic–3] and further blended with the microwave sol-gel samples in the weight ratio of 20:80. The mixtures were then heated to 1073 K before absorption studies. Fig. 4(a & b) present the TEM images of Eutectic 3 sample obtained after the heat treatment process. The rod morphology of the sample is well maintained with thickness varying from 40 nm to 100nm. The XRD pattern presented in Fig. 4c confirmed the presence of ortho and meta silicates of lithium in addition to the alkali silicate phases of Na and K. A comparative evaluation of the dynamic absorption isotherms of sol-gel[26], unmodified microwave sol-gel and microwave sol-gel samples modified with eutectic powder mixtures are presented in Fig. 4d. It is clear that the addition of eutectic mixtures increased the absorption capacity at low-temperature ranges of 623-823 K significantly. In the unmodified samples, the rate of absorption was very low in the initial absorption step (<823 K) compared to the second absorption step. However, in the samples containing the eutectic mixtures the absorption rate in the initial step was comparable to that of the second absorption step. In samples, Eutectic-1 and Eutectic - 2, two absorption steps are clearly visible as in the case of the unmodified sample. This is attributed to the carbonate shell formation, although a softer one compared to the unmodified sample, in these two cases. However, in the case of Eutectic-3 sample the two steps have combined to form a more or less single step absorption curve.

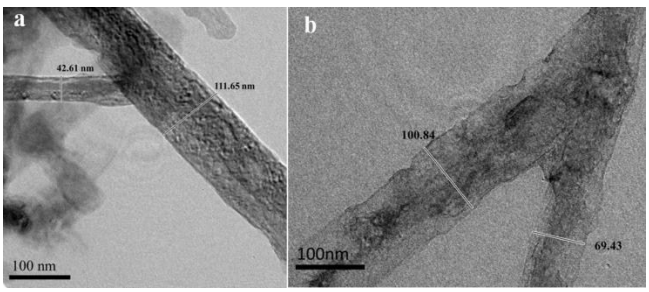

View Article Online
DOI: 10.1039/C6TA06133H

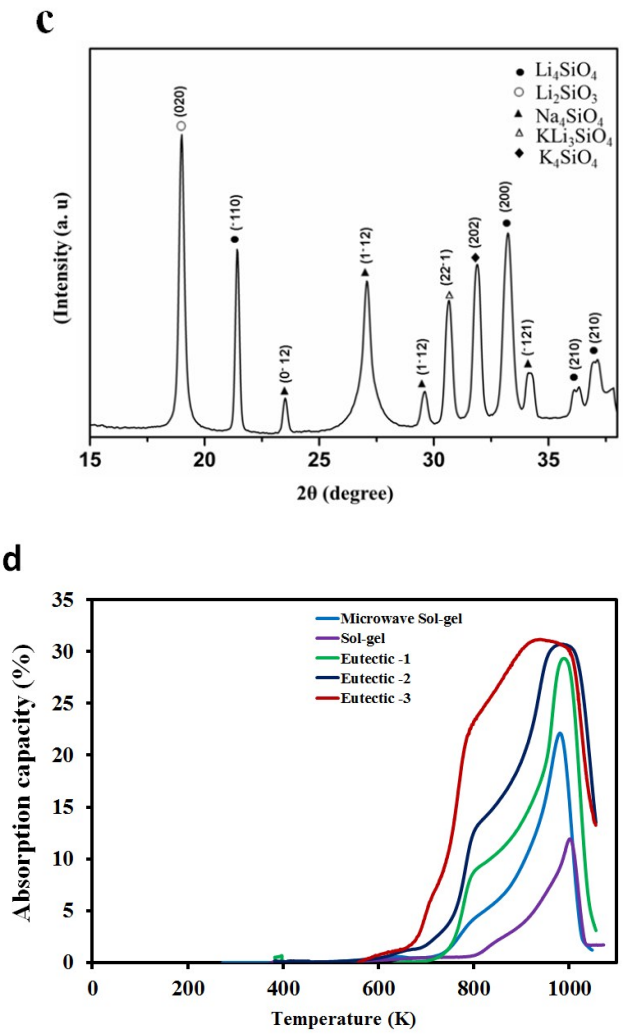

Fig.4 TEM images (a & b) of the Eutectic-3 particles (c) X-ray diffraction patterns of Eutectic-3 [Li_4SiO_4, JCPDS 37- 1472], (Li_2SiO_3, JCPDS 29-0828), (Na_4SiO_4, JCPDS 072-0185), (KLi_4SiO_4, JCPDS 038-0015),(K_4SiO_4, JCPDS 046-0601)].(d) Dynamic absorption curves of sol-gel, microwave sol gel as well as Eutectic 1, 2 & 3 samples.

Detailed results of the CO_2 absorption performance of the sample (Eutectic-3) at temperatures of 623-923 K are shown in Fig. 5a. As shown, absorption capacity as high as 35% could be observed at the temperature of 923 K. It should be noted that the amount of CO_2 adsorbed was higher than the value expected based on the stoichiometry of reaction of one CO_2 molecule with one orthosilicate available in the Eutectic-3 sample (See Fig. 4c & Fig. 5a). It is possible that the reaction might have continued till silica is formed (instead of Li_2SiO_3) at least in some of the fractions of the powder mixture. Further studies are required to fully understand the chemisorption mechanism of these samples.

Enhanced absorption rate was observed at temperatures as low as 623 K. Fig. 5b has a good comparison of the absorption rates of the Eutectic-3 sample with unmodified microwave and sol-gel[26] samples (calculated for the first 2 minutes of absorption). The rate of absorption observed for the Eutectic-3 sample, 0.28 wt. % sec^{-1} at 923 K, was significantly higher than the absorption rates measured with unmodified microwave sol-gel and sol-gel samples. A comparison of reported results (as shown in ESI S1) including the most recent literature also shows that the absorption performance of the sample is exceptional. The CO_2 absorption value of the sample, in fact, reached >30wt% within the first 42 seconds itself, based on which the absorption rate could be calculated as 0.72 wt. % sec^{-1}.

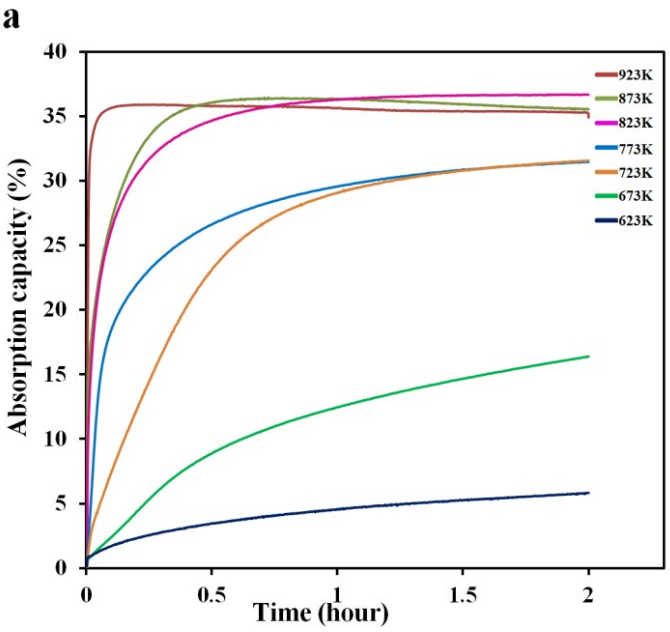

View Article Online
DOI: 10.1039/C6TA06133H

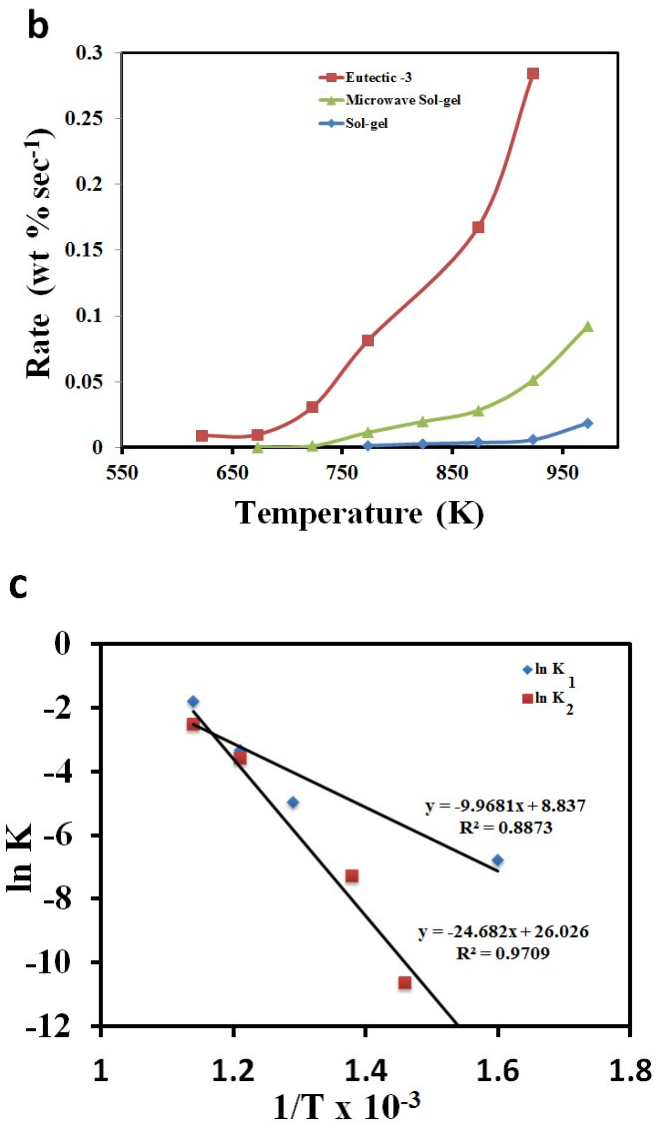

Fig.5 (a) CO_2 absorption curves of eutectic mixture (Eutectic-3) at various temperatures. (b) Absorption rates of Eutectic-3 at different temperatures (Rate values calculated from the initial two minutes of absorption curve) in comparison to microwave sol-gel and sol-gel samples. (c) Graph of lnK versus 1/T for the two different processes of chemisorption (K_1) and diffusion (K_2) observed for the Eutectic -3 sample.

In order to find out the rate determining steps, the absorption curves (Fig.5a) were fitted to the double exponential model and the resulting kinetic parameters were used to derive the Arrhenius plots as in Fig. 4c (further details are included in section S5 of Supplementary). It should be noted that K_1 values are larger in this case compared to K_2 values and is contrary to the behaviour of the microwave unmodified samples. However, this is attributed to the presence of eutectic phases in the modified samples, which is supposed to enhance significantly the chemisorption rates. As a result, even with the more or less similar particles sizes, modified and unmodified samples have different reaction limitations leading to the entire absorption process. The activation energy values calculated from Fig.5c were 82.3 kJ/mol and 205.18 kJ/mol for chemisorption and diffusion processes respectively. The activation energy for chemisorption process was found much lower than the diffusion process. The size of sodium and potassium ions are larger compared to the lithium ions and, therefore, the whole diffusion process could be restricted in this case.

Cyclic absorption-desorption performances for 15 cycles at 948 K using 100% CO_2 & 100% N_2 gases were performed and the results are shown in Fig. 6a. As shown, the sample retained > 95% (33.6 wt %) of its original absorption capacity even after 15 cycles at this very high temperature. Nevertheless, some structural and morphological changes are suspected as the shape of the absorption curve changed from the near perfect rectangle to smoothened edges as the number of cycles increased. Further improvement in the stability of the powders may be necessary and techniques like the addition of rare-earth second phases as reported by us recently may be required[30]. As shown here and in Fig. 5a, the sample showed absorption capacity of ~35% for absorption temperatures >823 K when the partial pressure of CO_2 gas was 1atm (100 % CO_2). Fig. 6b shows the comparative absorption curves of Eutectic-3 at 873 K for the CO_2 partial pressure values of 1 atm (100% CO_2) and 0.15 atm (15% CO_2 / 85% N_2). It is clear that the sample is capable of absorbing CO_2 to >25 wt % within the first few minutes of absorption even at the reduced CO_2 partial pressure of 0.15 atm.

View Article Online
DOI: 10.1039/C6TA06133H

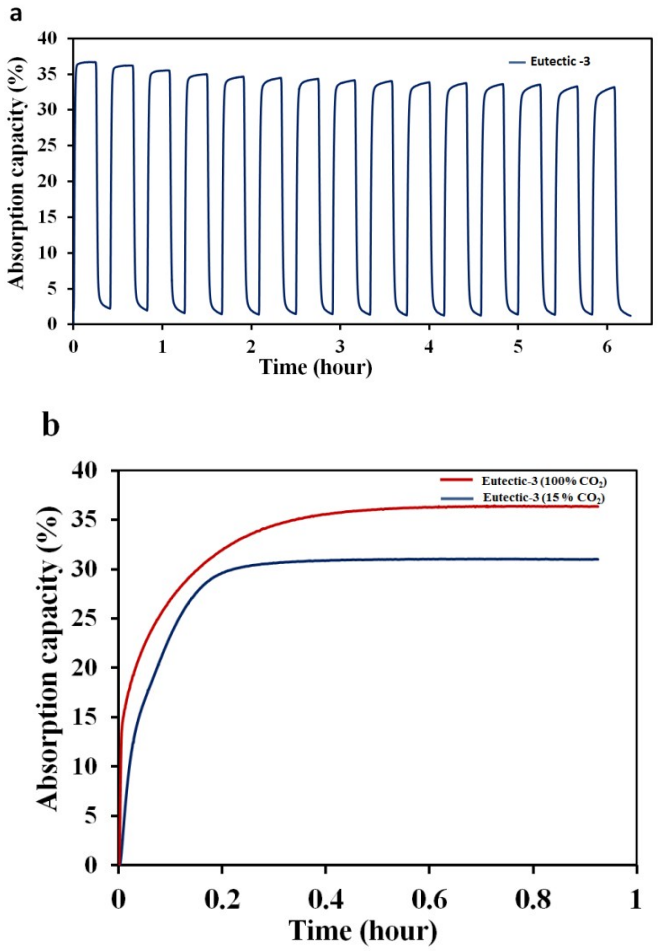

Fig. 6(a) Cyclic absorption-desorption performance of Eutectic-3 (Absorption was carried out at 948 K and desorption at the same temperature by changing 100% CO_2 to 100% N_2 gas). (b) Comparison of absorption curves of Eutectic-3 with 100% CO_2 flow and with 15% CO_2 flow. Absorption was carried out at 873K (15 % CO_2 or 100 % CO_2).

It should be noted that 15% CO_2 represents the composition of CO_2 containing product streams in several high-temperature chemical reactions as well as flue gases in power plantsand therefore the results indicate the possibility of using these materials for practical applications. This exceptional absorption behavior of Eutectic-3 should be due to the morphological as well as compositional features of this sample. With regard to kinetics and CO_2 absorption capacity, these morphology and composition tailored particles outperform other structured lithium silicate particles reported in the recent literature (Data from literature is shown in the section S1 of ESI).

3. Conclusions

In conclusion, a microwave assisted sol-gel synthetic approach is demonstrated for the synthesis of Li_4SiO_4 particles with nanorod morphology. The nanorods exhibited dramatically enhanced absorption rate of CO_2 along with exceptional durability. The nanorod morphology of the Li_4SiO_4 particles allowed ultrafast sorption kinetics due primarily to an easier surface reaction with CO_2 by virtue of shorter diffusion pathway for lithium from the bulk to surface of the rods. In addition, the large aspect ratio of the nanorods helped to enhance the durability of the particles by limiting their Ostwald ripening on high-temperature cyclic absorption/desorption loading. Further, we have modified the chemical composition of the Li_4SiO_4 particles by mixing with a eutectic mixture of K and Na. This compositional control of the materials helped to realize absorbents with extraordinary CO_2 absorption rates of 0.72 wt % sec^{-1} at 100% CO_2/923K. Cyclic absorption–desorption studies of these powder revealed that the materials remain durable up to 15 cycles without any significant reduction in CO_2 absorption capacity. Furthermore, the modified samples showed remarkable absorption performance at lower temperatures (573-823K) as well as lower CO_2 pressures (0.15 atm) demonstrating their potential in practical CO_2 separation applications.

Acknowledgements

The authors acknowledge the Council of Scientific and Industrial Research (CSIR), New Delhi, India, & Noritake Co. Limited, Aichi, Japan, for providing research facilities and financial support. Authors acknowledge Mr. Kiran Mohan for TEM and Dr. Bhoje Gowd & Mr. Prithviraj for XRD analyses.

Notes and references

1. M. Kato, S. Yoshikawa, K. Nakagawa, *J. Mater. Sci. Lett*,2002, **21**, 485-487.

2. J.Wang, L. Huang, R. Yang, Z. Zhang, J. Wu, Y. Gao, Q. Wang, D. O'Hare, Z. Zhong, Energy Environ. Sci, 2014, **7**, 3478-3518.

3. B. N. Nair, R. P. Burwood, V. J. Goh, K. Nakagawa, T. Yamaguchi, *Prog. Mater. Sci*,2009, **54**, 511-541.

4. D. M. D'Alessandro, B. Smit, J. R. Long, *Angw. Chem. Int. Ed*, 2010.**49**, 6058-6082.

5. L. Joos, K. Lejaeghere, J. M. Huck, V. Van Speybroeck, B. Smit,*Energy Environ. Sci*, 2015,**8**, 2480-2491.

6. M. Zaman, J. H. Lee, *Korean J.Chem. Eng*,2013, **30**, 1497-1526.

7. A. Samanta, A. Zhao, G. K. H. Shimizu, P. Sarkar, R. Gupta, *Ind. Eng. Chem*.**51**, 1438-1463 (2012).

8. J. Ortiz-Landeros, I. C. Romero-Ibarra, C. Gomez-Yanez, E. Lima, H. Pfeiffer, *J. Phys. Chem. C*, 2013, **117**, 6303-6311.

9. B. N. Nair, T. Yamaguchi, H. Kawamura, S. I. Nakao, K. Nakagawa, *J. Am. Ceram. Soc*,2004, **87**, 68-74.

10. C. Wang, Y. Chen, Z. Cheng, X. Luo, L. Jia, M. Song, B. Jiang, B. Dou, *Energy Fuels*, 2015, **29**, 7408-7418.

11. M. S. Yancheshmeh, H. R. Radfarnia, M. C. Iliuta, *Chem. Eng. J*, 2016, **283**, 420-444.

12. Y. Duan, H. Pfeiffer, B. Li, I. C. Romero-Ibar, D. C. Sorescu, D. R. Luebke and J. W. Halley, *Phys. Chem. Chem. Phys*. 2013, **15**, 13538-13558.

13. H. Xu, W. Cheng, X. Jin, G Wang, H. Lu, H. Wang, D. Chen, B. Fan, T. Hou, R. Zhang, *Ind. Eng. Chem*, 2013.**52**, 1886-1891.

14. T. Yamaguchi, T. Niitsuma, B. N. Nair, K. Nakagawa, *J. Membr. Sci*.2007, **294**, 16-21.

15. R. Rodriguez-Mosqueda, H. Pfeiffer, *J. Phys. Chem. A*, 2010, **114**, 4535-4541.

16. K. Wang, X. Guo, P. Zhao, F. Wang, C. Zheng, J. Hazard. Mater. 2011, **189**, 301-307.

17. J. Du, L. R. Corrales, *J. Mater. Chem. B*, 2006,**110**, 22346-22352.

18. K. Essaki, M. Kato, H. Uemoto, *J. Mater. Sci*,2005, **40**, 5017-5019.

19. M. Seggiani, M. Puccini, S. Vitolo, *Int. J. Greenhouse Gas Control***,**2011, **5**, 741-748.

20. H. Kim, H. D. Jang, M. Choi, *Chem. Eng. J*.2015, **280**, 132-137.

21. J. H. Lee, B. Moon, T. K. Kim, S. Jeoung, H. R. Moon, *Dalton Trans.* 2015,**44**, 15130-15134.

22. K. Wang, X. Y. Wang, P. F. Zhao, X. Guo, *Chem. Eng. Technol*,2014, **37**, 1552-1558.

23. S. Shan, S. Li, Q. Jia, L. Jiang, Y. Wang, and J. Peng, *Ind. Eng. Chem. Res*. 2013, **52**, 6941-6945.

24. V. L. Mejı´a-Trejo, E. Fregoso-Israel, *Chem. Mater*,2008, **20,** 7171-7176.

25. R. Quinn, R. J. Kitzhoffer, J. R. Hufton, T. C. Golden, *Ind. Eng. Chem. Res*.2012, **51**, 9320-9327.

26. P. V. Subha, B. N. Nair, P. Hareesh, A. Peer Mohamed, T. Yamaguchi, K. G. K. Warrier, U. S. Hareesh,*J. Mater. Chem. A*, 2014,**2**, 12792-12798.

27. H. Pfeiffer, P. Bosch, S. Bulbulian, Synthesis of lithium silicates. *J. Nucl. Mater*,1998, **257**, 309-317.

28. B. N. Nair, K. Keizer, T. Okubo, S. I. Nakao, *Adv. Mater*, 1998,**10**, 249-252.

29. M. J. Venegas, E. Fregoso-Israel, R. Escamilla, H. Pfeiffer, *Ind. Eng.Chem. Res*. 2007, **46**, 2407-2412.

30. P. V. Subha, B. N. Nair, P. Hareesh, A. Peer Mohamed, T. Yamaguchi, K. G. K. Warrier and U. S. Hareesh, *J. Phys. Chem. C*,2015,**119**, 5319-5326.

31. G. Cao, Nanostructures & Nanomaterials. Synthesis, Properties and Applications, Imperial College press London 2004.

32. M. Prokesova & Z. Panek, *Ceram. Int*, 1989, **15,** 369-374.